Numerical Study of a Three Dimensional Interaction between two bow Shock Waves and the Aerodynamic Heating on a Wedge Shaped Nose Cone

N Wu[1,*], J H Wang[1] and L Shen[1]

[1]Department of Thermal Science and Energy Engineering, School of Engineering Science, University of Science and Technology of China, Hefei 230027, Anhui, China

[*]nanwu@mail.ustc.edu.cn

Abstract. This paper presents a numerical investigation on the three-dimensional interaction between two bow shock waves in two environments, i.e. ground high-enthalpy wind tunnel test and real space flight, using Fluent 15.0. The first bow shock wave, also called induced shock wave, which is generated by the leading edge of a hypersonic vehicle. The other bow shock wave can be deemed objective shock wave, which is generated by the cowl clip of hypersonic inlet, and in this paper the inlet is represented by a wedge shaped nose cone. The interaction performances including flow field structures, aerodynamic pressure and heating are analyzed and compared between the ground test and the real space flight. Through the analysis and comparison, we can find the following important phenomena: 1) Three-dimensional complicated flow structures appear in both cases, but only in the real space flight condition, a local two-dimensional type IV interaction appears; 2) The heat flux and pressure in the interaction region are much larger than those in the no-interaction region in both cases, but the peak values of the heat flux and pressure in real space flight are smaller than those in ground test. 3) The interaction region on the objective surface are different in the two cases, and there is a peak value displacement of 3 mm along the stagnation line.

1. Introduction

Shock-shock interactions in hypersonic flight may cause extremely high aerodynamic heating, which will lead to the failure of thermal protection systems. For an SSTO (Single-Stage to Orbit) vehicle, the maximum heat flux of the cowl leading edge reaches up to 579MW/m^2 due to a type IV shock-shock interaction [1]. Besides the heating problem, the research on the flow field structures of shock/shock interactions is also an interesting problem. Edney [2] conducted a series of experiments on the two-dimensional interaction between a bow shock wave and a planar oblique shock wave, and classified the interactions into six types, among which the type IV induces the most intense heating around the interaction region.

After Edney [2], many further studies have been conducted on shock-shock interactions both in experimental and numerical aspects [3-6]. However, most of the investigations are limited within two-dimensional problems, mainly focusing on the two-dimensional type IV interaction or the three-dimensional interaction between a planar oblique and a bow shock wave. In real situations, the interaction between the bow shock generated by vehicle front and the bow shock of inlet cowl lip

shows three-dimensional effects. Therefore, it is significant to understand the real three-dimensional performances.

Before a real hypersonic flight, to validate a new thermal protection system, ground high-enthalpy wind tunnel tests are necessary. In the ground test, stagnation temperature is usually seen an important factor. To create the same stagnation temperature to real space flight, one has to use a lower Mach number but higher static temperature and pressure in ground high-enthalpy wind tunnel testes. Therefore, differences exist between the two environments. However, a few literatures mentioned the differences before this work, especially with the consideration of shock/shock interactions. To understand the differences of the two cases better, numerical simulation as an effective tool is used in this investigation. The aim is to investigate the flow field and the aerodynamic heating caused by the three-dimensional interaction, and to reveal the differences between the ground high-enthalpy wind tunnel test and the real space hypersonic flight.

2. Physical model

To simulate the typical three-dimensional interaction between the two bow shock waves generated by vehicle front and inlet cowl clip, the simplified physical model used in this paper is shown in figure1. It consists of two parts, a shock wave generator with a 10mm radius and a compression angle of 23 °to freestream direction, an objective nose cone with a radius of 5mm and a cone angle of 12 ° and an extension length of 80mm. The model is symmetrical and has a 2mm gap in horizontal direction.

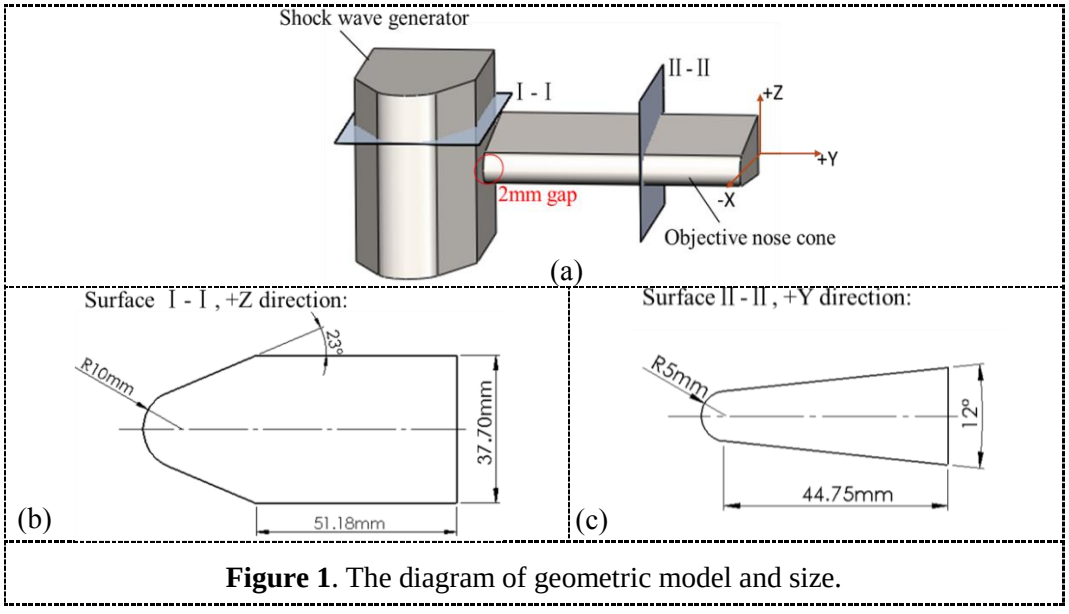

Figure 1. The diagram of geometric model and size.

3. Numerical method

3.1. Mesh setup

The mesh is generated by ICEM, and the computational domain is extended by ten times of the size of the model. Using the symmetrical condition, half of the model is built in order to save computation time. Here, non-uniform structured grid is used, and the grid near the wall is locally refined. After the validation of grid independence and mesh adaption, the grid strategy with about 4.5 million elements is used considering the balance of computational load and accuracy.

3.2. Solution strategies

Steady state assumption and Spalart-Allmaras turbulent model are used in the following simulations with Fluent 15.0 as the CFD solver. The differential equations are discretized using second–order

upwind scheme. The calculations are performed using density-based, coupled implicit method. The gas parameters are calculated by "Ideal gas model" and Sutherland formula. The inlet boundary condition of main flow is set by "pressure far-field" and at the exit by "pressure outlet". The wall of the model is set as adiabatic with no slip condition.

3.3. Calculation conditions

At the same stagnation temperature 2400K, the calculation conditions in ground test and real space flight are listed in Table 1, and the atmosphere parameters are computed by the formulas presented by the United States in 1976 [7].

Table 1. Calculation conditions in two cases.

Parameters	Mach number	Altitude	Total temperature	Static Temperature	Static Pressure
Values	4.2	Ground	2400K	530.035K	15030Pa
	7	26.5km	2400K	222.034K	2304Pa

4. Results and discussion

Using the parameters shown in Table 1, numerical simulations are carried out in the two cases, and the results including flow field, aerodynamic pressure and heating are analyzed and compared.

4.1. Flow field

Figure 2 shows Mach number contours in a horizontal section passing through the stagnation line and four vertical sections in ground test, among which section D represents the no-interaction region. In section A and B, as shown in figure 2b and 2c, we can see the shock location is far away from the stagnation point. In section C, as shown in figure 2d, there is a discontinuity between the objective nose cone and the objective shock wave. This phenomenon is caused by the induced bow shock wave, which divides the flow behind the shock wave into two direction flows, along the free stream and the span wise flow of the objective nose cone. The same three-dimensional complicated flow structures can also be seen in space flight condition.

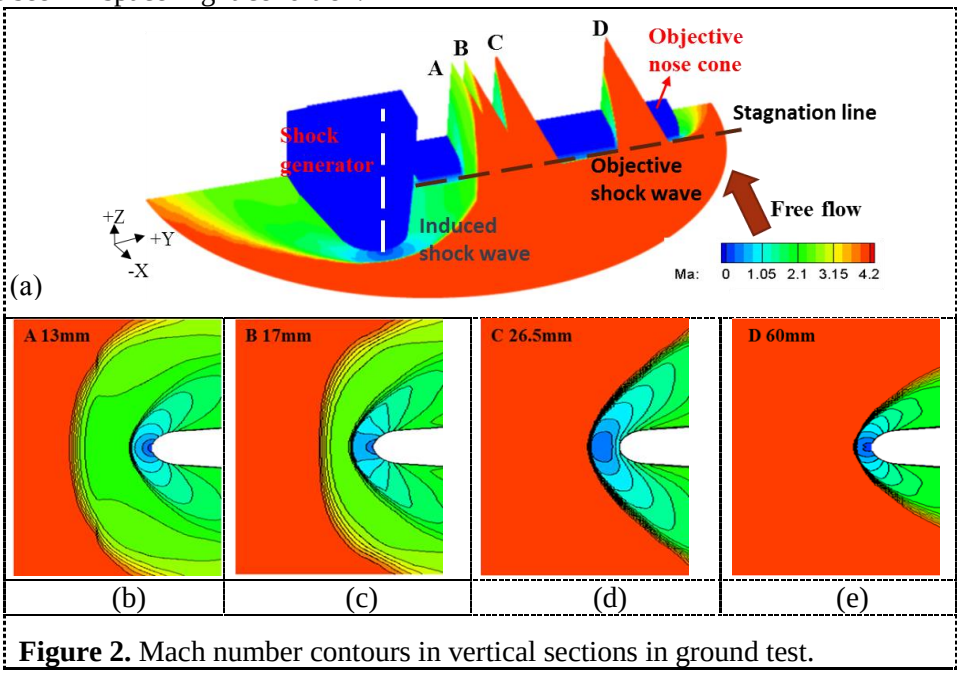

Figure 2. Mach number contours in vertical sections in ground test.

Figure 3 further exhibits the flow field in a horizontal section (z=0) in detail both in the ground test and real space flight. From this figure, we can find that: 1) In the two cases, near the nose cone surface, there is a shear layer, which is generated by the interaction of the induced shock wave with the

objective shock wave. In this shear layer, a local boundary layer separation and reattachment exist. 2) Only in the real space flight condition, a local supersonic region (Ma>1) appears inside the boundary layer, as shown in figure 3b. Now the interaction type is called as type IV shock wave by Edney [1]. The difference in flow field can be explained by the fact that: at the same stagnation temperature, the Mach number in the ground test is smaller than and the induced shock intensity is lower than that in the real high space, and therefore in the ground test there is no supersonic region, as shown in figure 3a.

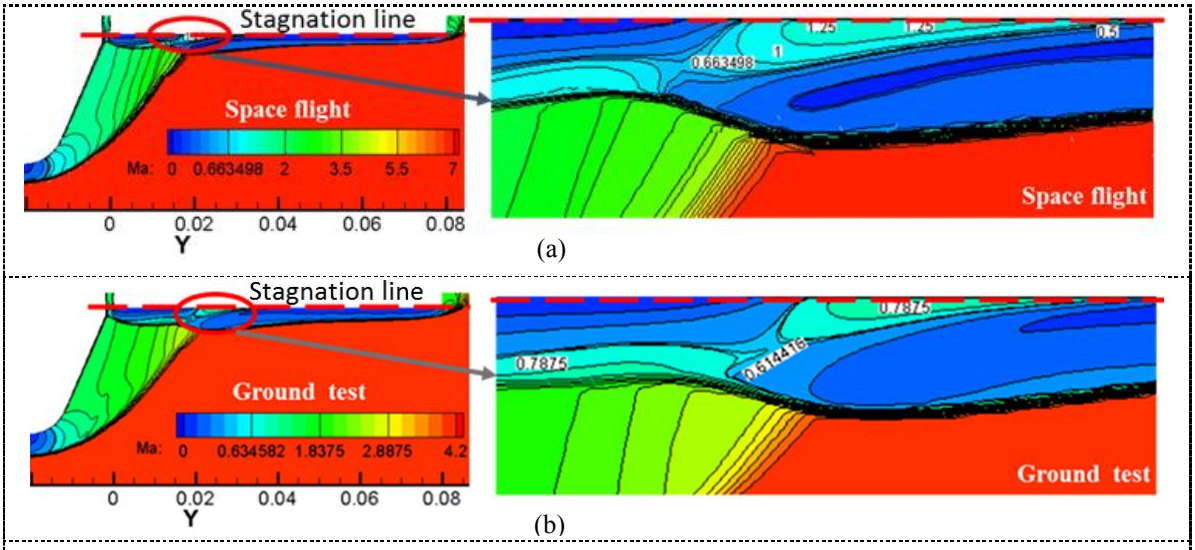

Figure 3. Mach number contours in horizontal section (z=0) in ground wind tunnel test and real space flight.

4.2. Aerodynamic pressure load

Figure 4a shows the pressure distribution in the stagnation region of the objective nose cone, and figure 4b further displays the pressure distribution along the stagnation line (the dashed red line shown in figure 4a).

From the analysis and comparison of the figures, we can find the following three interesting phenomena: 1) Pressure increases in the interaction region in both cases. 2) For the ground test, the peak value in the interaction region is 0.63MPa, about 1.8 times of the no-interaction region and 42 times of the inlet pressure (0.015MPa). However the peak value for the space flight is about 0.28 MPa, which is much lower than that in the ground test. 3) The peak value is at Y=18mm along the stagnation line in the ground test, and Y=15mm in the space flight. There is a difference of 3mm along the stagnation line in y direction between the two cases. The reason is that to achieve the same stagnation temperature 2400K, Mach number is 4.2 in the ground test, which is much smaller than Ma=7 in the space flight. Accordingly, the angle of the Mach cone in the ground test is larger and the interaction region moves farther along the extension direction.

The above phenomena indicates that in active thermal protection systems, to cool the stagnation area or nose cone, for the real space flight, the driving force to inject cooling media is much lower than that in the ground test, and the driving force in the shock-shock interaction region is larger than that of the no-interaction region in both cases.

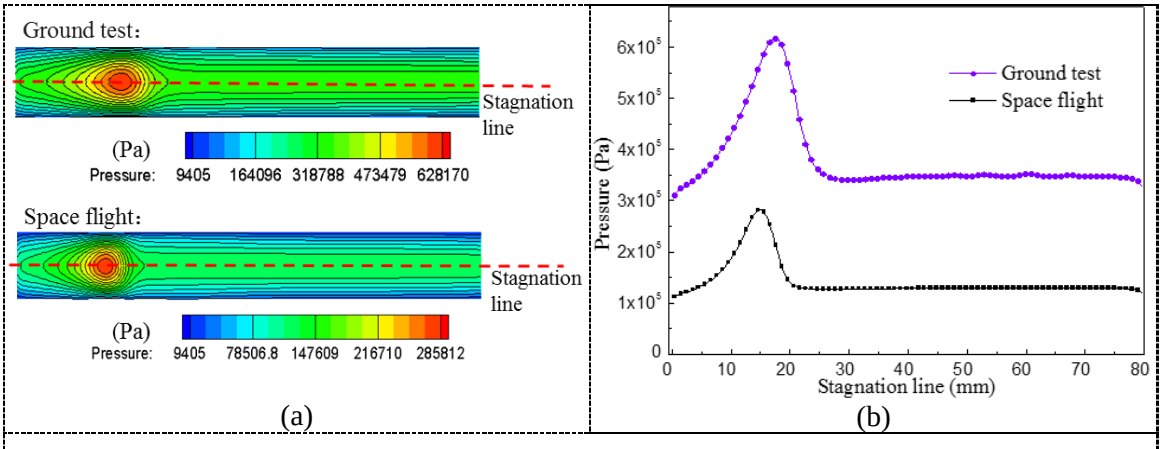

Figure 4. Pressure distribution of the nose cone along the stagnation line in ground wind tunnel experiment and real space flight.

4.3. Aerodynamic heating

Here, the adiabatic temperature boundary condition is replaced using a constant temperature of 280K and the aerodynamic heating on the objective nose cone is investigated. Figure 5 shows the heat flux distribution along the stagnation line, the dashed red line shown in figure 4a.

Through figure 5, one can find the following phenomena: 1) Heat flux increases in the interaction region in both cases. 2) The peak heat flux in the ground test is much larger than that in the space flight. For the ground test, the peak heat flux reaches to 17.76MW/m^2, which is about 1.6 times of the no-interaction region. While for the real space flight, the maximum heat flux is close to 11.94 MW/m^2, about 1.93 times of the no-interaction region. This can be explained by the fact that though the stagnation temperature and the wall temperature are set the same in the two cases, the Reynold number of the free flow in the ground test is much larger, and the local heat transfer in the interaction region is more intense. 3) Comparing the heat flux distribution with the pressure distribution as shown in figure 4, we can find that they have the same location of the peak value in the two cases.

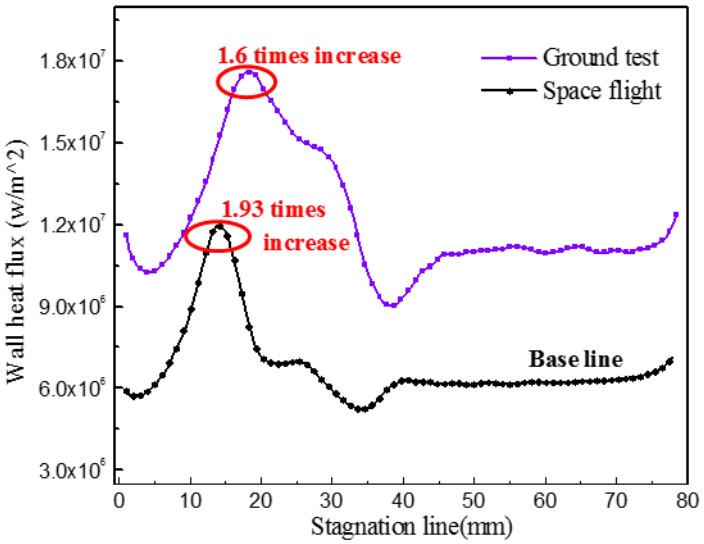

Figure 5. Wall heat flux distribution along the stagnation line in ground test.

5. Conclusions

A numerical investigation is carried out to study the three-dimensional interaction of two bow shock waves at two conditions, ground high-enthalpy wind tunnel test and real space flight. The differences of flow field and aerodynamic characteristics between the two cases are analyzed and compared. Through the analysis and comparison, the following conclusions can be drawn:

1) Three-dimensional complicated flow structures appear in both cases, but only in the real space flight a local two-dimensional type IV shock wave appears in the horizontal section.
2) At the same stagnation temperature, the pressure and heat flux in the interaction region are much larger than those in the no-interaction region in both cases, but the peak values in the real space flight are much smaller than those in the ground test, which means that the thermal environment is more severe in ground tests.
3) At the same stagnation temperature, the peak values of the heat flux and pressure occupy the same location in both cases. But the interaction regions are different in the two cases, and there is a peak value displacement of 3 mm along the stagnation line. It's a good guidance for the design of thermal protection systems.

6. References

[1] Glass D E 2008 Ceramic matrix composite (CMC) thermal protection systems (TPS) and ho structures for hypersonic vehicles *15th AIAA Space Planes and Hypersonic Systems and Technologies Conf.* (Dayton) pp 1-36
[2] Edney B 1968 Anomalous heat-transfer and pressure distribution on blunt bodies at hypersonic speeds in the presence of an impinging Shock(Sweden:Stockholm) *FFA* **No 115**
[3] Duquesne 1998 Numerical investigation of a three dimensional turbulent shock/shock interaction *AIAA 36th Aerospace Sciences Meeting & Exhibit* (NV.: Reno)
[4] Nowak R J and Holden M S 1990 Shock/Shock Interference on a Transpiration Cooled Hemispherical Model *AIAA 21st Fluid Dynamics, Plasma Dynamics and Lasers Conf.* (WA: Seattle)**Vol 1**
[5] Wieting A R and Holden M S 1989 Experimental Study on Shock Wave Interference Heating on a Cylindrical Leading Edge at Mach 6 and 8 *AIAA Journal* **Vol. 27** pp1557-1565
[6] Miyaji K 1999 Numerical analysis of three-dimensional shock/shock interactions and the aerodynamic heating *37th Aerospace Sciences Meeting and Exhibit* (NV:Reno)
[7] Lin J and Wang J H 2014 Numerical Investigation on Aero-Thermodynamic Characteristics of Wedge Shaped Nose Cone of Near Space Supersonic Flight *In Applied Mechanics and Materials* **vol 541** pp 608-612

Acknowledgements

This work is supported by the National Natural Science Foundation of China (No. 51376168) and the 3rd Institute of China Aerospace Science and Industry Corp.